PION AND KAON DISSOCIATION IN THE NUCLEAR COULOMB FIELD*

D. Berg, C. Chandlee, S. Cihangir, T. Ferbel, J. Huston, T. Jensen, F. Lobkowicz, C. A. Nelson[#]
T. Ohshima, P. Slattery and P. Thompson
University of Rochester, Rochester, N.Y. 14627

J. Biel, T. Droege, A. Jonckheere and P. F. Koehler
Fermi National Accelerator Laboratory, Batavia, IL. 60510

S. Heppelmann, T. Joyce, Y. Makdisi[†], M. Marshak, E. Peterson, K. Ruddick, T. Walsh and J. Whittaker
University of Minnesota, Minneapolis, MN. 55455

(Presented by T. Jensen)

SUMMARY

We have investigated the diffractive and Coulomb dissociation of pions and kaons from nuclear targets. The experiment was performed in the M-1 beam line of the Meson Area of Fermilab. Data were obtained at 156 GeV/c and at 260 GeV/c. We report a measurement of the radiative width of the ρ^-, and first estimates of the radiative widths of the $K^*(890)^-$ and A_2^-.

We are reporting on our study of coherent dissociation of pions and kaons into their corresponding vector and tensor mesons in the Coulomb field of nuclear targets. In particular, we use the Primakoff effect in the reaction $\pi^-A \to \rho^-A$ to extract the radiative width $\Gamma(\rho^- \to \pi^-\gamma)$[1].

An outstanding problem in this field has been the small value of 35 ± 10 keV measured for $\Gamma(\rho^- \to \pi^-\gamma)$[2]. If we interpret the reaction $\rho^- \to \pi^-\gamma$ in terms of a quark model, then the decay process can be regarded as a radiative transition from a $^3S_1$ state to a $^1S_0$ state of the $q\bar{q}$ system. Transitions of this kind can be calculated to yield relations between various radiative widths. For example, assuming ideal singlet-octet mixing for the vector-meson nonet, the radiative transitions of the ω^0 and ρ^- can be related to yield $\Gamma(\rho^- \to \pi^-\gamma)/\Gamma(\omega^0 \to \pi^0\gamma) \sim 1/9$.[3] **Using the directly measured width of 880 ± 60 KeV for the decay $\omega^0 \to \pi^0\gamma$,[4] yields an experimental ratio 1/25 for the ρ to ω radiative widths, rather than the value of 1/9.**

Backgrounds from strong-exchange processes (in particular ω exchange) complicate the analysis of the ρ^- production data. However, as the energy of the incident beam is increased the analysis becomes cleaner because the Primakoff cross section increases as $\ell n\, p$, whereas the strong process falls as $1/p$. The previous measurement of $\Gamma(\rho^- \to \pi^-\gamma)$ was obtained at 23 GeV/c, where strong exchange is important. We have performed our experiment at 156 GeV/c and 260 GeV/c where the Primakoff process dominates ρ^- production at small momentum transfers.

Figure 1 displays schematically the high-resolution forward spectrometer which we have set up in the M1 beamline at Fermilab. Charged-particle trajectories are measured with arrays of drift chambers located on either side of an analyzing magnet that provides a 1 GeV/c transverse impulse. The resolution of the chambers is ±200 μ. Energies and positions of photons are measured by a lead-liquid argon shower detector, which has positional resolution of better than ±1 mm and an energy resolution $\Delta E/E$ of about $\pm 13\%/\sqrt{E}$.

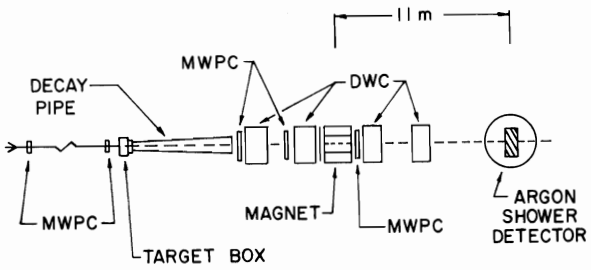

Fig. 1. Schematic of the high-resolution forward spectrometer for Experiment E272.

The incident beam was tagged using three Cerenkov counters, and the incident angles were determined to ±.03 mrad with two sets of proportional chambers located upstream of the target.

The target was surrounded by lead-scintillator veto counters to enhance the coherent contribution to the trigger. The target and veto counters were contained within an evacuated box which was directly connected to a 6m. long decay pipe. This enabled us to trigger on "Vee" decays in the vacuum region and provided a clean sample of $K^- \to \pi^-\pi^0$ events which we used to monitor the performance of our apparatus, and to establish the normalization for our measurement of cross sections.

Figure 2 provides an indication of the resolution of our spectrometer at 156 GeV/c. The data are from K^- decays accumulated during runs using a lead target that was 0.28 radiation lengths thick.

A typical $\pi^-\pi^0$ mass distribution for our data is shown in Fig. 3. For these data we required that the reconstructed production vertex be at the target position, the total energy be equal to the beam energy, and the mass of the two detected photons be equal to the π^0 mass. The $\pi^-\pi^0$ mass distribution is clearly dominated by the ρ^- meson. The acceptance of the equipment as a function of mass is indicated by the smooth curve and is typically about 60%.

The absolute reconstruction efficiency for π^0 mesons in the liquid argon calorimeter is uncertain to about ±13%. We have consequently normalized our production cross sections to the observed $K^- \to \pi^-\pi^0$ decays that we accumulate along with our data. Because a π^0 from the decay of a K^- has characteristics very similar to that of a π^0 from the decay of a ρ^-, normalizing to K^- decays eliminates this and many other

*Research supported by the U.S. Department of Energy, The National Science Foundation and the Universities of Minnesota and Rochester.
[#]Presently at Fermi National Accelerator Laboratory.
[†]Presently at Brookhaven National Laboratory.

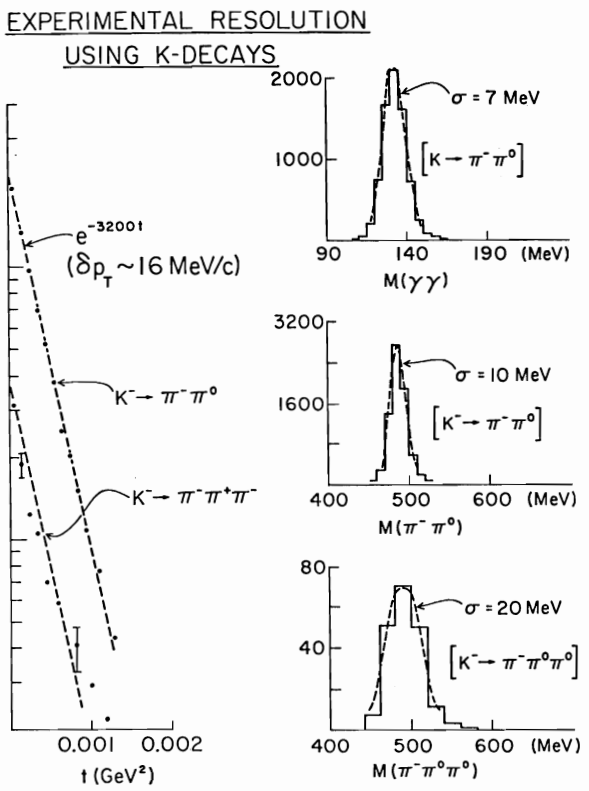

Fig. 2. Resolution studies at 156 GeV/c, using K^- decays from data with a lead target of 0.28 radiation lengths.

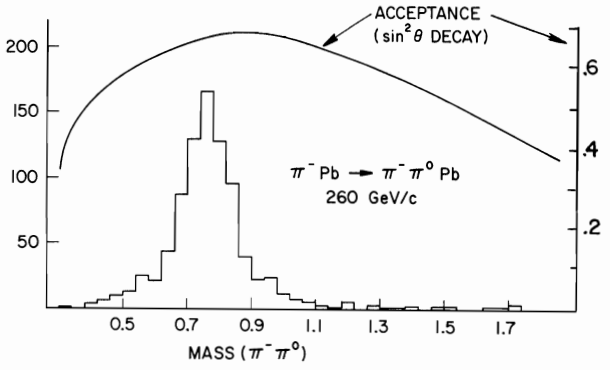

Fig. 3. Typical two-pion mass spectrum for events satisfying total energy, target vertex and π^0-mass cuts. The Monte Carlo generated acceptance is indicated by the solid curve. The data are for 260 GeV/c π^- mesons incident on a lead target.

systematic problems. To check that our procedure is valid we have examined the ratio of the ρ^- yield to the $K^- \to \pi^-\pi^0$ yield as a function of the helicity decay angle of the $\pi^-\pi^0$ system. The results are shown in Fig. 4 for data for three different targets. These plots have been corrected for background (target empty) and for the K^-/ρ^- relative geometrical acceptance. Because K^- mesons decay isotropically, a characteristic $\sin^2\theta$ dependence is expected in Fig. 4 due to the M-1 nature of ρ^- production. This is indeed what is observed in the data.

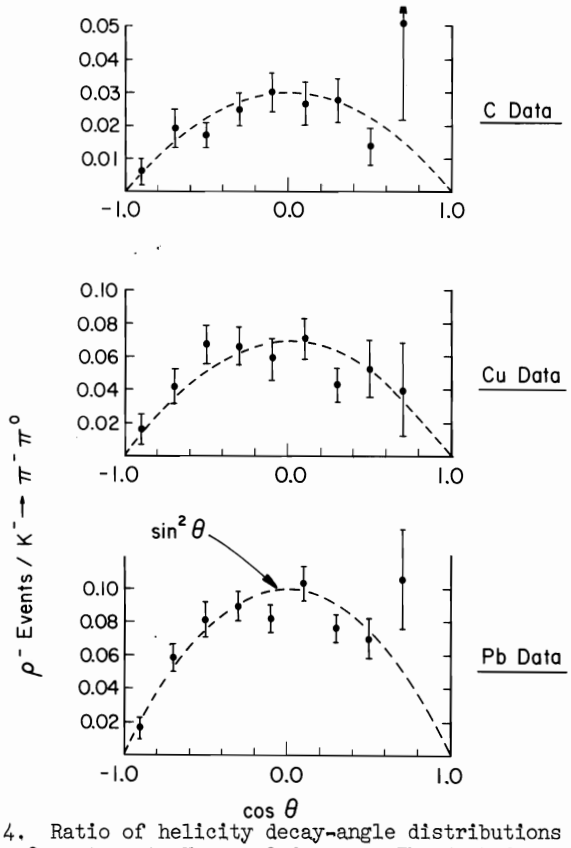

Fig. 4. Ratio of helicity decay-angle distributions for $\pi^-\pi^0$ systems to $K^- \to \pi^-\pi^0$ decays. The dashed curves show the $\sin^2\theta_\pi$-dependence expected for ρ^- mesons.

As a further check of our normalization procedure we compared our data for $pPb \to p\pi^0Pb$ to that expected for Primakoff production on the basis of the reaction $\gamma p \to p\pi^0$. The $p\pi^0$ mass spectrum, normalized to K^- decays, is shown in Fig. 5; the solid line shows the cross section expected from the Primakoff contribution (mainly $\Delta(1236)$) on the basis of recent photoproduction data[5]. Below 1.25 GeV agreement with the data is good to better than 5%. Our data show an excess in the high mass region which can be qualitatively understood in terms of strong diffractive production of $p\pi^0$ systems in the I = ½ state.

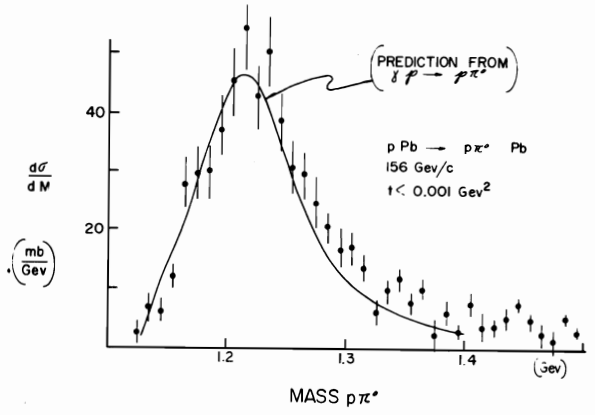

Fig. 5. $p\pi^0$ mass spectrum for coherent Δ^+ production on lead. The solid line shows the prediction for Primakoff production based on recent photoproduction data (Ref. 5).

With these tests satisfied, we are confident that we can proceed to extract the radiative width of the ρ^- from our data. If ρ^- production were purely electromagnetic the cross section would be determined by the Coulomb amplitude F_c:

$$\frac{d^2\sigma_{EM}}{dtdM^2} = |F_c|^2 = \frac{Z^2\alpha}{\pi}\,\frac{t-t_{min}}{t^2}\,\frac{|F_{EM}(t)|^2}{M^2 - m_\pi^2}\,\sigma_\gamma(M^2), \qquad (1)$$

where α is the fine structure constant, Z the nuclear charge, and M the mass of the dipion system. The square of the minimum four-momentum transfer is t_{min}, and $F_{EM}(t)$ is the electromagnetic form factor for the nucleus(including absorption).

$$\sigma_\gamma(M^2) = \frac{6\pi M^2}{(M^2 - m_\pi^2)^2}\,|T(\gamma\pi \to \pi\pi)|^2 \qquad (2)$$

is the cross section for the reaction $\gamma\pi \to \pi\pi$. We assume that the T-matrix has the form of a p-wave Breit-Wigner resonance:

$$|T(\gamma\pi \to \pi\pi)|^2 = \frac{M_o^2\Gamma_{\gamma\pi}(M^2)\Gamma_{\pi\pi}(M^2)}{(M^2 - M_o^2)^2 + M_o^2\Gamma_{\pi\pi}(M^2)}\ , \qquad (3)$$

where $\Gamma_{\pi\pi}$ and $\Gamma_{\gamma\pi}$ are the mass-dependent full and radiative widths, and M_o is the mass at resonance.

We have used different phenomenological forms for the partial widths, such as:

$$\Gamma_{\pi\pi} = \Gamma_o\,\frac{q^3}{q_o^3}\,\frac{2q_o^2}{q_o^2 + q^2} \qquad (4)$$

$$\Gamma_{\gamma\pi} = \Gamma_{\gamma o}\,\frac{k^3}{k_o^3}\,\frac{2k_o^2}{k_o^2 + k^2}\ , \quad \Gamma_{\gamma o}\,\frac{k^2}{k_o^2}\,\frac{2k_o^2}{k_o^2 + k^2}$$

In these expressions q and k are the momenta in the rest frame of the $\pi\pi$ and $\gamma\pi$ system respectively. Values at resonance are subscripted with a zero. We find that, although fits of different forms to the data differ in the χ^2, the various forms do not markedly affect the values of the parameters at resonance. Two such fits to the ρ mass spectrum are shown in Fig. 6, where the arrows indicate the region over which the fits were performed. The best fit yields $M_o = 776 \pm 4$ MeV and $\Gamma_o = 149 \pm 8$ MeV, in good agreement with the accepted values[4].

The ω-exchange contribution to ρ^- production can be parameterized as:

$$\frac{d\sigma_H}{dt} = |F_S|^2 = A^2C_S|t-t_{min}||F_H(t)|^2, \qquad (5)$$

where A is the atomic mass number, C_S gives the normalization for production on a single nucleon, and $F_H(t)$ is the hadronic form factor for the nucleus.

These two processes can interfere, and we can write the cross section in the form

$$\frac{d\sigma}{dt} = |F_C + e^{i\phi}F_S|^2\ , \qquad (6)$$

where ϕ is the relative phase of the Coulomb and strong amplitudes. The parameters $\Gamma_{\gamma o}$, C_S and ϕ were varied in a fit of the data to the above expression. The fits are shown in Fig. 7 for three targets, and the resulting parameters for several typical fits are given in Table I.

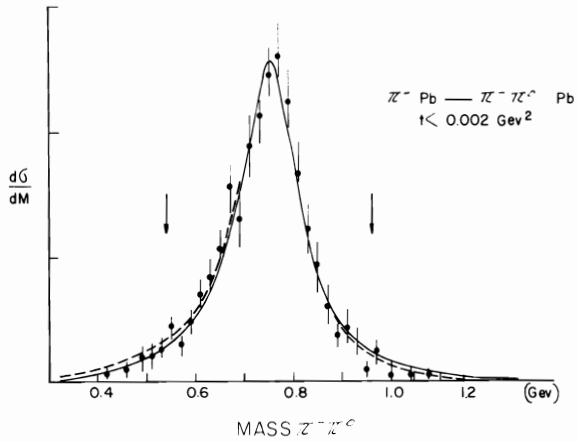

Fig. 6. $\pi^-\pi^0$ mass spectrum for coherent ρ^- data on lead, at small momentum transfers. Fits to the spectrum were performed using the data between the incicated arrows; various forms were assumed for the parameterization of partial widths. Two such fits are plotted here and the best fit yields $M_o = 776 \pm 4$ MeV and $\Gamma_o = 149 \pm 8$ MeV for the mass and width of a p-wave ρ^- line shape.

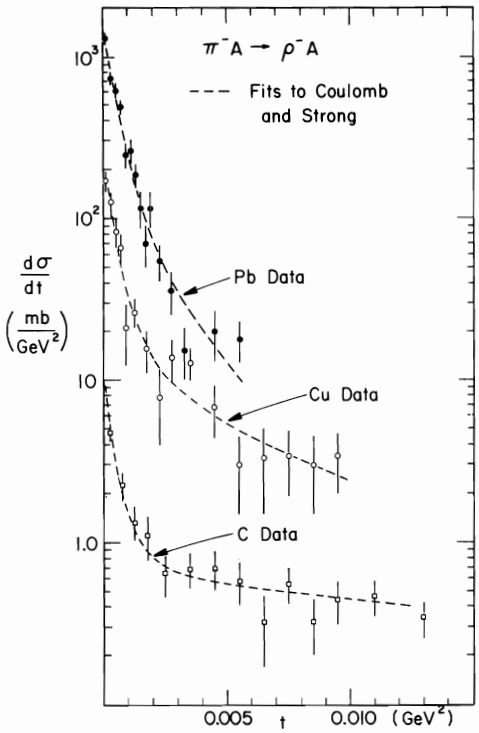

Fig. 7. t-distributions for coherent ρ production on Pb, Cu, and C targets at 156 GeV/c. The dashed lines are fits of the data to equation (6).

For each target we find two solutions that differ mainly in the value for the phase ϕ and C_S.[6] If we combine data from all targets we obtain the results given in the third set of entries in Table 1. In addition to statistical errors from the fit, we estimate a systematic error of ±7 keV on $\Gamma_{\gamma o}$ due to uncertainty in our normalization procedure. From our fits we conclude that $\Gamma_{\rho \to \pi\gamma} = 63 \pm 7$ keV.

Table I. Typical Results of Fits to t-Distributions at 156 GeV/c

	Lead		Copper		All Targets	
	Solution I	Solution II	Solution I	Solution II	Solution I	Solution II
Γ_{γ_o} (KeV)[a]	70 ± 3	62 ± 3	62 ± 5	59 ± 4	65 ± 2	61 ± 2
C_S (mb/GeV^4)	0.4 ± 0.2	1.9 ± 0.6	0.7 ± 0.2	1.0 ± 0.2	0.76 ± 0.06	0.84 ± 0.08
ϕ	68 ± 25	-90 ± 15	41 ± 25	-63 ± 20	52 ± 11	-52 ± 12
χ^2/DOF	1.2	1.4	1.0	1.0	1.3	1.3

(a) Errors are statistical; the systematic uncertainty is ±7 KeV.

In addition to the ρ measurement, we have preliminary data on several states of higher mass. Figure 8 shows the signal for coherent K*(890) production, combining both $K^{*-} \to K^-\pi^o$ and $K^{*-} \to K^o_S\pi^-$ decay modes. Evidence for $A_2 \to \pi^-\eta$ is shown in Fig. 9. We observe a sharp forward Coulomb peak in the t-distribution and the characteristic $\sin^2\theta\cos^2\theta$ angular distribution expected for the decays of electromagnetically produced A_2 mesons. Finally, Fig. 10 shows the first clear evidence for Coulomb production of the A_1.

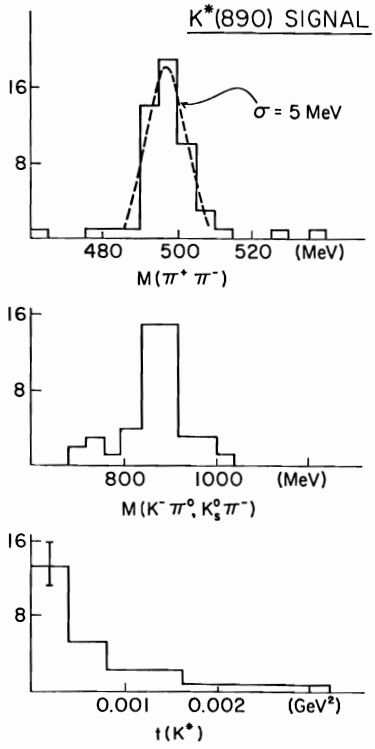

Fig. 8. Data from an analysis of coherent K*⁻(890) production. a) $\pi^+\pi^-$ mass from $K^o_S \to \pi^+\pi^-$ decays from $K^*(890) \to K^o_S\pi$. b) Combined mass spectrum from $K^-\pi^o$ and $K^o_S\pi^-$ decay modes. c) t-distribution for coherent K*⁻(890) events.

In conclusion, we summarize in Table II our measurements of the radiative widths of vector and tensor mesons.

Acknowledgments

We thank Drs. T. Toohig, A. Brenner, A. Greene, A. Wehman, and T. Yamanouchi of Fermilab for their support and interest in our experiment.

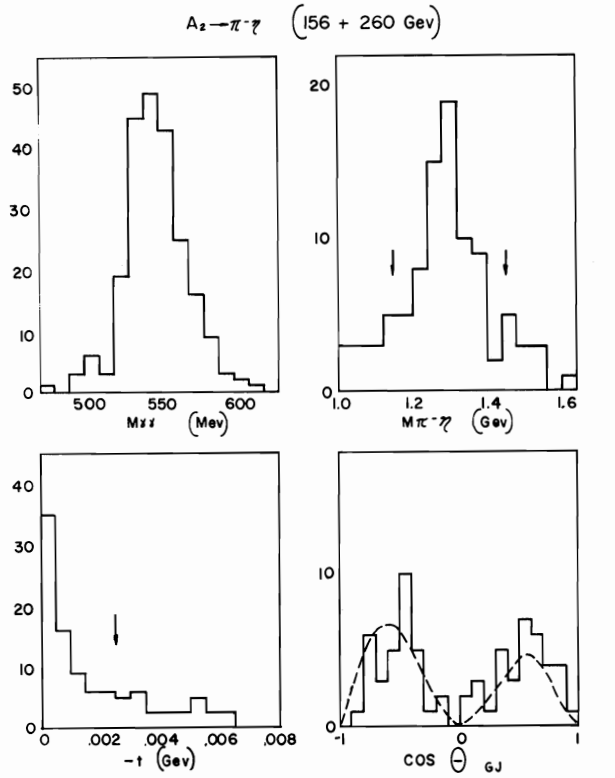

Fig. 9. Data from an analysis of coherent A_2 production. a) η signal from γγ mass combinations. b) A_2^- signal in the $\pi^-\eta$ mode. c) The t-distribution for coherent A_2^- production. d) Polar decay-angle distribution of the π^- from A_2^- decay, for $t < 0.0025$ GeV^2 calculated in the Gottfried-Jackson frame.

Table II. Summary of latest results from Experiment E272.

Process	Γ_{γ_o} (KeV)
$\rho^- \to \pi^-\gamma$	63 ± 7
$K^*(890)^- \to K^-\gamma$	40 ± 15
$A_2^- \to \pi^-\gamma$	450 ± 100
$A_1 \to \pi^-\gamma$	observed

A_1 SIGNAL

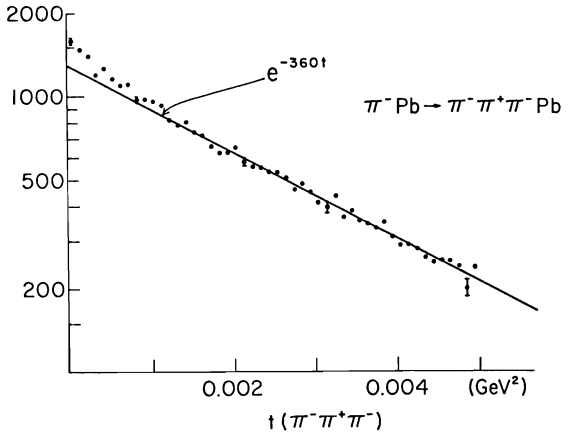

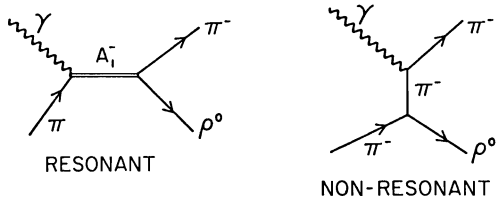

Fig. 10. t-distribution for $\pi^-\pi^+\pi^-$ systems with an invariant mass between .80 GeV and 1.5 GeV, produced on a lead target. Only a fraction of the Coulomb peak at small t ($\lesssim 0.001$ GeV^2) can be attributed to A_2^- production.

References

1. See, for example, G. Fäldt, Nucl. Phys. B43, 591 (1972), and references given therein to earlier work.
2. B. Gobbi, et al., Phys. Rev. Letts. 33, 1450 (1975); ibid, 37, 1439 (1976).
3. See, for example, C. Becchi and G. Morpurgo, Phys. Rev. 140B, 687 (1965).
4. Particle Data Listings, Phys. Letts. 75B, No. 1 (1978).
5. G. Fischer et al, Nucl. Phys. B16, 93 (1970) and R. L. Walker, Phys. Rev. 182, 1729 (1969).
6. We are presently expanding the fits to the data to include additional background terms in the hope of eliminating the ambiguities due to the two solutions.